Spin nematic ordering in the spin-1 chain system

A. A. Zvyagin[1,2,3] and V. V. Slavin[1,3]

[1]*B.I. Verkin Institute for Low Temperature Physics and Engineering of the National Academy of Sciences of Ukraine, Nauky Avenue 47, Kharkiv 61103, Ukraine*

[2]*Max-Planck Institut für Physik komplexer Systeme, Nöthnitzer Straße 38, D-01187 Dresden, Germany*

[3]*V.N. Karazin Kharkiv National University, 4 Svoboda square, Kharkiv 61022, Ukraine*

(Received 8 June 2022; revised 14 July 2022; accepted 1 August 2022; published 24 August 2022)

We predict the instability of the quantum spin-1 chain material with respect to the spin nematic ordering. For the spin subsystem the spin nematic order parameter is related to the onset of single-ion spin anisotropy. The ordering is caused by the coupling to the elastic subsystem of the crystal or, for spin-1 ultracold bosons in a one-dimensional optical lattice, by the interaction with a Bose-Einstein condensate. Our conclusions are based on the exact integrability of the spin model and on numerical simulations for the nonintegrable cases. Our exact results also describe the behavior of interacting gluons within the lattice toy Yang-Mills-like model, in which spontaneous and field-induced symmetry breaking can be realized.

DOI: 10.1103/PhysRevB.106.054429

I. INTRODUCTION

Among other "hot" topics the search for new states of condensed matter, in particular, in interacting electron systems, attracts the attention of researchers. The nematic state, similar to the ordered phases of molecules in liquid crystals [1], is one of the most intriguing examples of such new states of electron systems. Instead of, e.g., magnetic ordering, in which the (dipolar) spin vector order parameter breaks the time-reversal T symmetry, in nematic states a distinguished orientation is developed, i.e., the order parameter is a director there [2]. The preferred orientation implies the rotation O(3) symmetry breaking. Such a nematic ordering was studied in heavy-fermion systems [3], in rare-earth insulators [4], and in some iron-based superconductors [5–9]. Usually, such a nonconventional ordering is connected with electron correlations, related to the exchange coupling together with weaker (mostly relativistic) interactions.

For magnetic systems the spin nematic ordering was studied theoretically [10–12]. Often the emergence of the spin nematic ordering is related to the geometrical frustration of the spin lattice, which suppresses the standard magnetic (spin-dipolar) ordering [13–15]. Spin nematicity is related to the spin multipoles, e.g., to the nonzero components of the expectation values of the second-rank spin traceless quadrupolar tensor $Q^{\alpha\beta} = S^{\alpha}S^{\beta} + S^{\beta}S^{\alpha} - [S(S+1)/3]\delta_{\alpha\beta}$, where S^{α} ($\alpha = x, y, z$) is the operator of the projection of spin S. For spin $S = 1/2$ only intersite spin nematic ordering can exist [16–18], while for higher values of S the single-site spin nematic ordering is possible. Despite many recent efforts (see, e.g., Refs. [19–21]), the experimental proof of the spin nematic ordering in magnets is still under question, because the spin nematic order parameter is not coupled to the external field directly. Also, while spin nematic ordering was studied phenomenologically [10,11], the microscopic theory of that phenomenon remains a challenge.

For $S \geqslant 1$ the spin nematic ordering was predicted for systems with the biquadratic spin-spin exchange interaction [22]. It is commonly believed that the biquadratic exchange is rather small in real magnetic materials. However, in experiments on ultracold atoms [23,24] and in a Ni-based magnetic material [25–27] there is evidence that the biquadratic exchange is present.

One-dimensional quantum systems are distinguished from other systems because for many one-dimensional systems exact quantum mechanical solutions are known [28]. Such an integrability permits theoretically exact characteristics of many-body quantum systems to be obtained. On the other hand, features of the one-dimensional density of states yield an enhancement of quantum and thermal fluctuations, which results in the destruction of the long-range ordering for quantum systems with gapless excitations for nonzero temperatures [29,30]. Instead, in the ground state, one-dimensional quantum systems (as a rule, those that have gapped excitations) manifest long-range ordering [31,32], with quantum phase transitions between ordered and disordered phases [33].

The goal of our present work is to investigate a one-dimensional quantum spin system coupled to the elastic subsystem of a spin chain material. Using the exact integrability of the spin subsystem and numerical simulations, we show that there can exist phase transitions to the spin nematic ordered phase, in which quadrupole spin ordering takes place. We study how the external magnetic field can affect such a spin nematic ordering. Using numerical methods, we consider the deviation from the exactly solvable model, studying that way-more-realistic situation, and investigate whether the spin nematic order persists for that case. The influence of nonzero temperature on the phase transition to the spin nematic ordered phase is also studied. Finally, as a by-product, using the exact solution, we consider the one-dimensional lattice model of interacting gluons, which results can be used in high-energy physics.

II. SPIN CHAIN MODEL

The Hamiltonian of the considered spin $S = 1$ chain model is

$$\mathcal{H} = \sum_n \big[J\mathbf{S}_n \cdot \mathbf{S}_{n+1} + J'(\mathbf{S}_n \cdot \mathbf{S}_{n+1})^2 - HS_n^z + D\big(O_2^0\big)_n\big], \qquad (1)$$

where $\mathbf{S}_n$ is the operator of the spin $S = 1$ in the nth site of the chain, J is the exchange parameter, J' is the parameter of the biquadratic exchange coupling, H is the external magnetic field (we use the units in which the effective magneton $g\mu_B = 1$, with g being the effective g factor and μ_B being the Bohr magneton), $(O_2^0)_n = (S_n^z)^2 - S(S+1)/3$ is the Stevens operator [28], related to the component of the spin quadrupole tensor, and D is the component of the (internal) field coupled to that Stevens operator (the parameter of the single-ion magnetic anisotropy). Generally speaking, for the isotropic exchange one can use any direction of the field H; using unitary transformations, one can reduce the situation to that of Eq. (1). (Notice that in what follows all numerical calculations are carried out in dimensionless units, so that $J = 1$.)

III. SU(3) SYMMETRIC SPIN-1 MODEL

The model described by Hamiltonian (1) is an exactly solvable SU(3) symmetric one at $J' = J$ (the Uimin-Lai-Sutherland model [34–36]). For the SU(3) symmetric spin model all components of the spin moment $\sum_n S_n^{x,y,z}$ and the Stevens operators $\sum_n (O_2^m)_n$ ($m = 0, \pm 1 \pm 2$) commute with the exchange part of the Hamiltonian; hence they have the same set of eigenfunctions. This is why it is convenient to classify all the states of the SU(3) symmetric Hamiltonian according to values of projections of the components of the SU(3) fields. In general, one can use any component of the SU(3) field in the SU(3) symmetric Hamiltonian; hence one can use any kind of Stevens operator $(O_2^m)_n$, which situation can be transformed to the case (1) for $J' = J$ by the unitary transformation.

Within the Bethe ansatz solution the eigenvalues and eigenfunctions of the SU(3) symmetric model are described by two sets of rapidities, $u_{j=1}^{n_a+n_b}$ and $v_{m=1}^{n_a}$. Here, $n_{a,b,c}$ with $a, b, c = \pm 1, 0$ are the numbers of states with each possible value of the z projection of the site spin S_j^z, i.e., $\pm 1, 0$. Obviously, one has $n_1 + n_0 + n_{-1} = N$, where N is the number of spins in the chain. It is assumed that $n_a \leqslant n_b \leqslant n_c$. For periodic boundary conditions the rapidities satisfy the following set of Bethe ansatz equations (BAEs):

$$(-1)^N X_1^{-N}(u_j) = \prod_{m=1}^{n_a} X_1(u_j - v_m) \times \prod_{q=1}^{n_a+n_b} X_2(u_j - u_q),$$
$$j = 1, \dots, n_a + n_b,$$
$$\prod_{b=1}^{n_a} X_2(v_m - v_b) = \prod_{q=1}^{n_a+n_{-b}} X_1(v_m - u_q),$$
$$m = 1, \dots, n_a, \qquad (2)$$

where $X_n(y) = (2y + in)/(2y - in)$. Taking the logarithm of the BAEs, one gets

$$N\tan^{-1}(u_j) - \sum_{q=1}^{n_a+n_b} \tan^{-1}([u_j - u_q]/2) + \sum_{m=1}^{n_a} \tan^{-1}(u_j - v_m) = \pi J_j,$$
$$\sum_{b=1}^{n_a} \tan^{-1}([v_m - v_b]/2) + \sum_{q=1}^{n_a+n_b} \tan^{-1}(u_q - v_m) = -\pi I_m, \qquad (3)$$

where J_j and I_m are integers or half-integers depending on the values of n_a and $n_a + n_b$. It was shown that

$$J_{j+1} - J_j = 1, \quad I_{m+1} - I_m = 1. \qquad (4)$$

The eigenvalue of the SU(3) symmetric Hamiltonian satisfying the BAEs is

$$E = J\left[N - \sum_{j=1}^{n_a+n_b} \frac{4}{4u_j^2 + 1}\right] - HM_z + DQ_z, \qquad (5)$$

where M_z and Q_z are the eigenvalues of the z projection of the total spin of the system, $\sum_n S_n^z$ and $\sum_n (O_2^0)_n$, respectively. The momentum of the state is

$$P = 2\pi\left(\sum_{j=1}^{n_a+n_b} J_j + \sum_{m=1}^{n_a} I_m\right) + \pi(n_a + n_b) \bmod 2\pi. \qquad (6)$$

It was shown that in the ground state for the antiferromagnetic case $J > 0$ in the thermodynamic limit $N, n_{a,b,c} \to \infty$ with the ratios $n_{a,b,c}/N$ fixed, the rapidities, which satisfy the BAEs, are real [34]. The equations for the densities of rapidities $\rho(u)$ and $\sigma(v)$ are

$$2\pi\rho(u) = a_1(u) - \int_{-A}^{A} dy a_2(u - y)\rho(y) + \int_{-B}^{B} dz a_1(u - z)\sigma(z),$$
$$2\pi\sigma(v) = \int_{-A}^{A} dy a_1(v - y)\rho(y) - \int_{-B}^{B} dz a_2(v - z)\sigma(z), \qquad (7)$$

where $a_1(x) = 4/(1+4x^2)$, $a_2 = 2/(1+x^2)$. The limits of integration are determined from the condition

$$\frac{n_a}{N} = \int_{-B}^{B} dy\sigma(y),$$
$$\frac{n_a+n_b}{N} = \int_{-A}^{A} dx\rho(x). \tag{8}$$

The energy is

$$E = N\left[J - \int_{-A}^{A} dx a_1(x)\rho(x)\right] - HM_z + DQ_z. \tag{9}$$

There are six combinations, connecting $n_{a,b,c}$ and $n_{\pm1,0}$ (i.e., the connections of $n_{a,b,c}$ with the values of M_z and Q_z).

(1) For $n_a = n_{-1}$ and $n_b = n_0$, we have $n_c = n_1 = N-(n_a+n_b)$, so that $M_z = N-(n_a+n_b)-n_a$ [i.e., $(M_z/N) = 1 - \int_{-A}^{A} du\rho(u) - \int_{-B}^{B} dv\sigma(v)$] and $Q_z = N-(n_a+n_b)+n_a-(2N/3)$ [i.e., $(Q_z/N) = (1/3) - \int_{-A}^{A} du\rho(u) + \int_{-B}^{B} dv\sigma(v)$]. This case is related to the situation of large positive values of the magnetic field H.

(2) For $n_a = n_{-1}$ and $n_b = n_1$, we have $n_c = n_0 = N-(n_a+n_b)$; hence $M_z = (n_a+n_b)-2n_a$, and $Q_z = (n_a+n_b)-(2N/3)$.

(3) For $n_a = n_0$ and $n_b = n_{-1}$, we have $n_c = n_1 = N-(n_a+n_b)$; hence $M_z = N-2(n_a+n_b)+n_a$, and $Q_z = (N/3)-n_a$.

(4) For $n_a = n_0$ and $n_b = n_1$, we have $n_c = n_{-1} = N-(n_a-n_b)$; hence $M_z = -N+2(n_a+n_b)-n_a$, and $Q_z = (N/3)-n_a$.

(5) For $n_a = n_1$ and $n_b = n_{-1}$, we have $n_c = n_0 = N-(n_a+n_b)$; hence $M_z = -(n_a+n_b)+2n_a$, and $Q_z = (n_a+n_b)-(2N/3)$.

(6) For $n_a = n_1$ and $n_b = n_0$, we have $n_c = n_{-1} = N-(n_a+n_b)$; hence $M_z = -N+(n_a+n_b)+n_a$, and $Q_z = N-(n_a+n_b)+n_a-(2N/3)$. This case is related to the situation of large negative values of the magnetic field H.

For the minimization of the energy at fixed values of D and H one has to minimize (9) with respect to $0 \leqslant A, B < \infty$ and $(M_z)_i$, $(Q_z)_i$. Here, the index $i = 1, 2, \ldots, 6$ enumerates possible combinations, connecting $n_{a,b,c}$ and $n_{\pm1,0}$ for given D and H.

Figure 1 shows the ground-state magnetic field behavior of the magnetic moment per site $m_z = N^{-1}M_z$ of the SU(3) symmetric model for various values of D. The curves in Fig. 1 are the numerical solutions of Eqs. (7)–(9). We see that the magnetic moment is the odd function of H for all values of D, as it must be. There is no spontaneous magnetization for any value of D. Depending on the strength of the field D (positive D describes the easy-plane situation, while negative D describes the easy-axis case), different behaviors of the magnetic moment persist. One can see several critical values of the field related to the lines of ground-state phase transitions [37–39] between the so-called SU(3) symmetric phase, SU(2) symmetric phases [39], spin-polarized phases, and large-D phases. For example, for $D = 0$ there are only two critical points, dividing the SU(3) symmetric phase (small values of H) with gapless excitations and the SU(2) symmetric phase (intermediate values of H with gapless excitations; for that case the states with $S_n^z = -1$ projection are absent) and dividing the SU(2) symmetric phase and the spin-polarized phase (high values of H in which only states with $S_n^z = 1$ with gapped excitations are present). Such a behavior persists for small enough values of positive D (the easy-plane case), while for large positive D the phase in which $S_n^z = \pm1$ states are absent with gapped excitations is also present. For the easy-axis case (negative D) there is a quantum phase transition between the SU(3) symmetric case and the spin-polarized case.

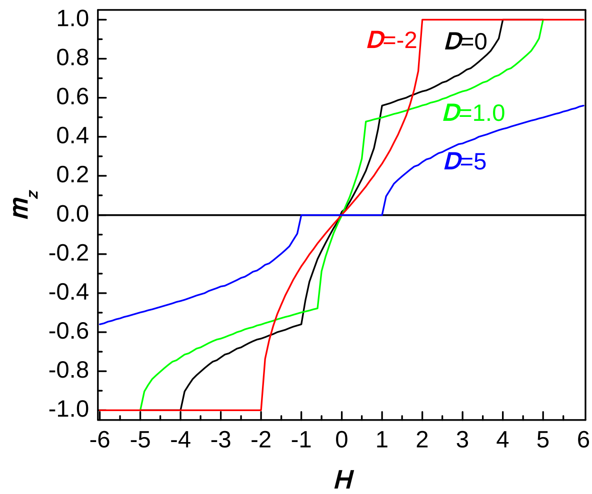

FIG. 1. The ground-state dependence of magnetic moment per site $m_z = N^{-1}M_z$ on magnetic field H of the SU(3) symmetric spin-1 chain for various values of the field D. (Recall that $J = J' = 1$.)

Figure 2 manifests the ground-state D dependence of the expectation value of the Stevens operator per site $q_z = N^{-1}Q_z$ of the SU(3) symmetric spin model for various values of the magnetic field H. That expectation value satisfies the relation $Q_z(H) = Q_z(-H)$. As in Fig. 1, Fig. 2 shows several critical values of D related to the lines of ground-state quantum phase transitions [39]. For example, for $H = 0$ the quantum phase transitions exist between the SU(3) symmetric phase and

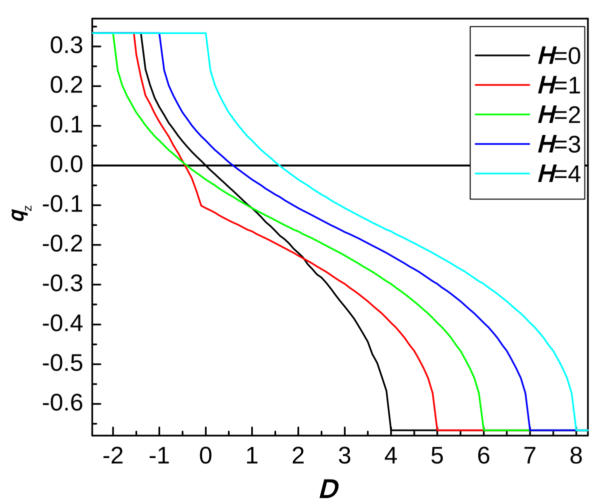

FIG. 2. The field D ground-state behavior of the Stevens operator $q_z = Q_z/N$ per site of the SU(3) symmetric spin-1 chain for various values of the magnetic field H.

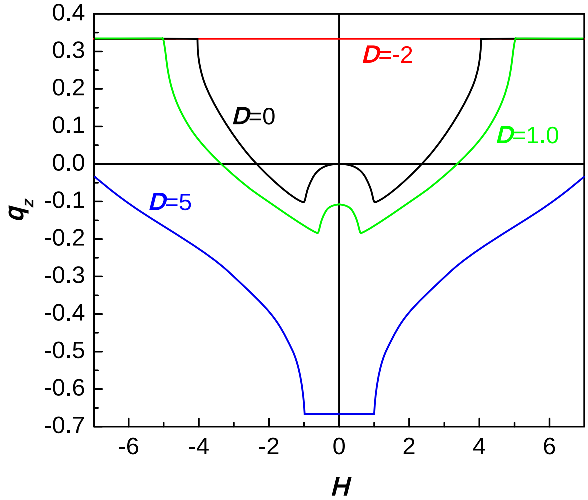

FIG. 3. The ground-state value of the Stevens operator per site $q_z = Q_z/N$ for various values of D of the SU(3) symmetric spin-1 chain as a function of the magnetic field H.

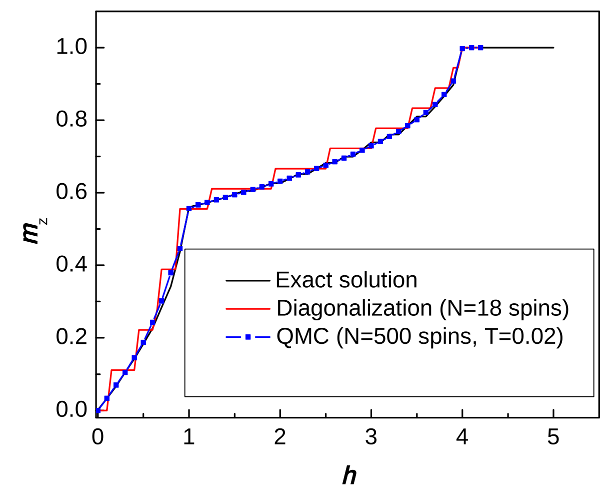

FIG. 4. The ground-state magnetic field behavior of the magnetic moment per site $m_z = M_z/N$ for $D = 0$: Comparison of exact results and numerical simulations (the exact diagonalization method and the quantum Monte Carlo method).

the phases with maximal and minimal values of q_z, namely, $q_z = 1/3$ and $q_z = -2/3$ with gapped excitations. The solution of Eqs. (7)–(9) shows that this transition takes place at $D = 4$, which coincides with the critical value of D obtained in Ref. [39]. For intermediate values of the magnetic field H, the quantum phase transition between the SU(3) symmetric phase and the SU(2) symmetric phase can also be seen. Notice that for $D = 0$ we have $q_z = 0$ in the absence of the magnetic field H, as it must be; the use of $(S_n^z)^2$ instead of the Stevens operator erroneously produces a nonzero spontaneous value of the quadrupole moment.

In Fig. 3 we show the expectation value of the Stevens operator q_z as a function of the applied magnetic field H for several values of the field D. First, it is seen that $q_z(H) = q_z(-H)$, i.e., the expectation value of the Stevens operator is the even function of the magnetic field for all values of D. For positive D (the easy-plane magnetic anisotropy) one can clearly see the nonmonotonic dependence. For example, for $D = 0$ at $H \leqslant J$ the value of q_z becomes smaller with the growth of H, while for $H \geqslant J$ it grows till $H = 4J$ (the quantum phase transition to the spin-polarized phase), and then for $H \geqslant 4J$ we obtain $q_z = 1/3$. Similar behavior persists for small positive values of D. For large positive D the expectation value is $q_z = -2/3$ for small values of H; then, at intermediate values of H, q_z grows with the increase in H till the critical value, above which $q_z = 1/3$. For the easy-axis case (negative values of D) the expectation value of the Stevens operator is constant, $q_z = 1/3$, for any value of the magnetic field H.

It should be noted that nonmonotonic dependencies of $q_z(D)$ and $q_z(H)$ (see Figs. 2 and 3) are explained by the phase transitions which take place in the system under consideration. This result is in full agreement with the phase diagram obtained in Ref. [39]. So, for example, breaks in dependencies $q_z(H)$ at $D > -2$ correspond to the transitions from the U-spin (or V-spin) phase (the notations of Ref. [39]) to the SU(3) phase (see Fig. 1 of Ref. [39]).

IV. OTHER VALUES OF THE BIQUADRATIC EXCHANGE COUPLING

To go beyond the integrable SU(3) symmetric spin-1 model, we have performed numerical calculations for the systems with different values of the biquadratic exchange interaction $J' \neq J$.

To check the correctness of the numerical procedures used, in Fig. 4 a comparison of the exact results and the results of numerical calculations (the exact diagonalization (see, e.g., Ref. [40]) and the quantum Monte Carlo (QMC) calculations (see, e.g., Refs. [41–43])) is shown. One can see that the results of numerical calculations agree very well with the exact ones.

Using the QMC method, we have calculated the expectation values of the magnetic moment (Fig. 5) and the Stevens operator (Figs. 6 and 7) for various values of the biquadratic exchange coupling J'. All the QMC simulations were carried

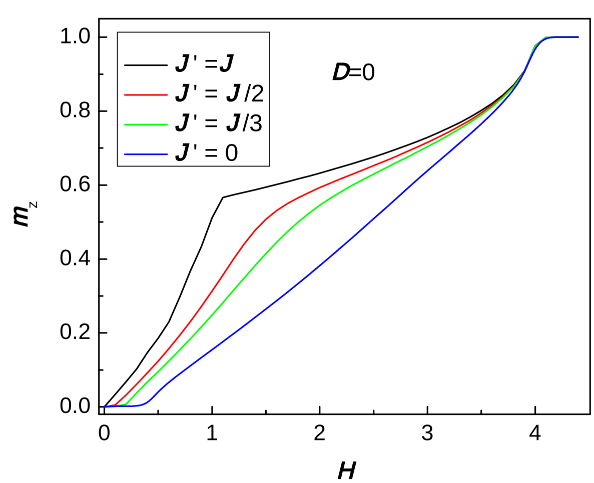

FIG. 5. The low-temperature dependence of the magnetic moment per site m_z on magnetic field H for several spin-1 chain models with various values of $J' \geqslant 0$ for $D = 0$.

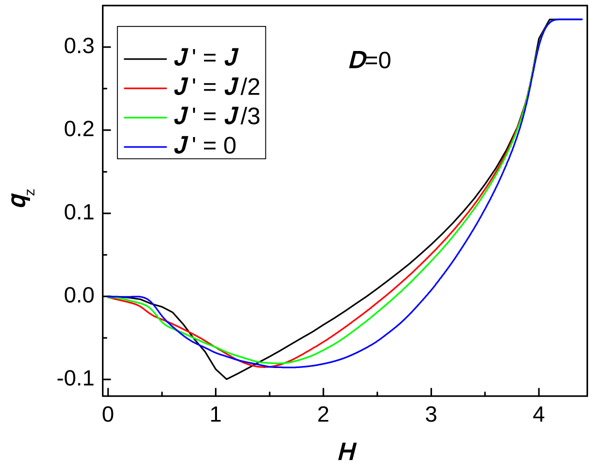

FIG. 6. The low-temperature dependence of the expectation value of the Stevens operator per site q_z on magnetic field H for several spin-1 chain models with various values of $J' \geqslant 0$ for $D = 0$.

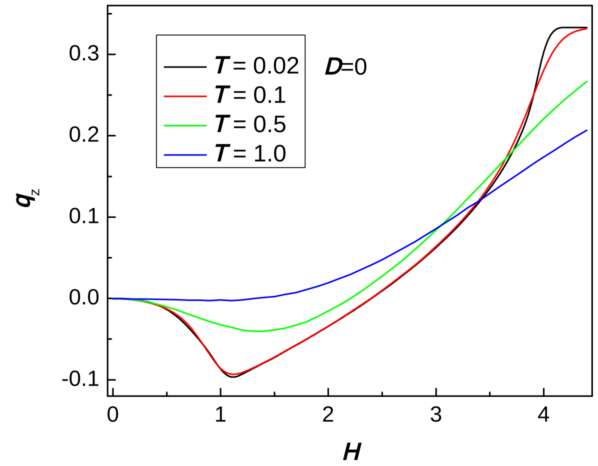

FIG. 8. The magnetic field behavior of the expectation value of the Stevens operator per site q_z at $D = 0$ for the SU(3) symmetric ($J' = J$) spin-1 chain for several values of the temperature T.

out for the chain of $N = 500$ spins at temperature $T = 0.02$. From Fig. 5 we see that for small values of the magnetic field H the gapped Haldane phase exists [44] for $J' \neq J$. Notice also the absence of the quantum phase transition between the SU(3) symmetric and the SU(2) symmetric phases for nonintegrable cases. Figure 6 manifests that the qualitative behavior of q_z as a function of the magnetic field at $D = 0$ persists for $J' \leqslant J$ (again, for small H the Haldane gap is seen, and there is no critical value of the magnetic field of the quantum phase transitions between two gapless regimes). However, it is clear that the behavior of the magnetic moment and the expectation value of the Stevens operator for the nonintegrable cases is reminiscent of their behavior for the integrable SU(3) symmetric situation. From Fig. 7 we see that for small negative values of the biquadratic exchange the situation is similar to the case of $J' \geqslant 0$. However, for larger values of J' the expectation value q_z grows monotonically with the increase in H until the critical value of H, above which $q_z = 1/3$. It is important to point out (see Figs. 6 and 7) that the external magnetic field H can cause the nonzero value of the Stevens operator (the spin nematic ordering) in the ground state for $D = 0$ for all values of the biquadratic exchange interaction.

Figures 8 and 9 show the QMC results for the magnetic field and temperature behavior of the expectation value of the Stevens operator per site q_z for the SU(3) symmetric case ($J' = J$). QMC results for the magnetic field behavior of q_z in the realistic case of $J' = 0$, in which only standard Heisenberg exchange is present, are shown in Fig. 10, and the results for the negative biquadratic coupling ($J' = -J/2$) are presented in Fig. 11. We see that the magnetic field dependencies for those cases are very similar (except for the low-temperature features of the Haldane phase and the absence of the transition between gapless phases). The low-temperature behavior of the SU(3) symmetric system agrees well with the ground-state behavior shown in Fig. 4. Notice that the use of the string hypothesis [45,46] within the Bethe ansatz for the integrable case $J' = J$ yields similar results. The low-temperature behavior of the free energy of the integrable model for gapless

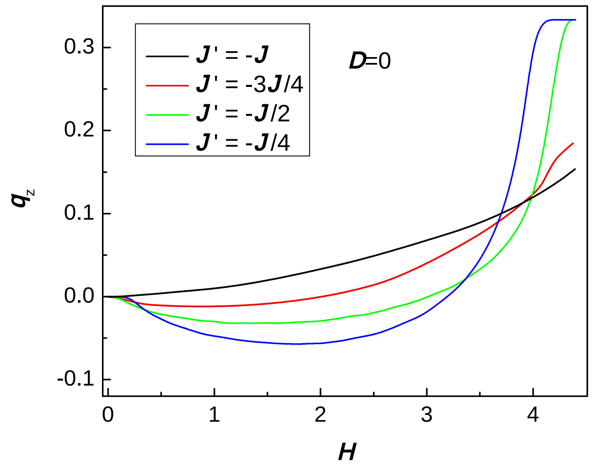

FIG. 7. The low-temperature dependence of the expectation value of the Stevens operator per site q_z on magnetic field H for several spin-1 chain models with various values of $J' \leqslant 0$ for $D = 0$.

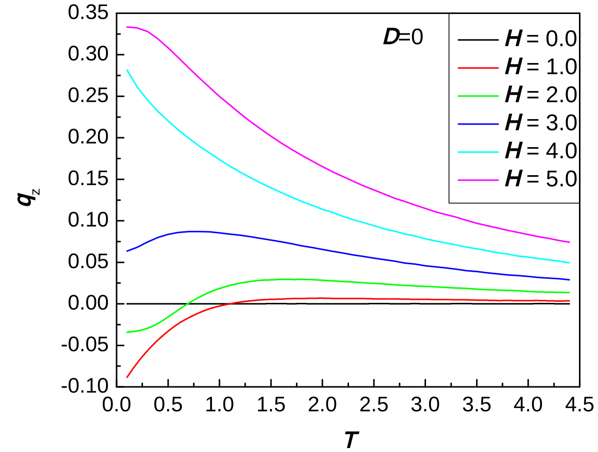

FIG. 9. The temperature dependence of the expectation value of the Stevens operator per site q_z at $D = 0$ for the SU(3) symmetric ($J' = J$) spin-1 chain for several values of the magnetic field H.

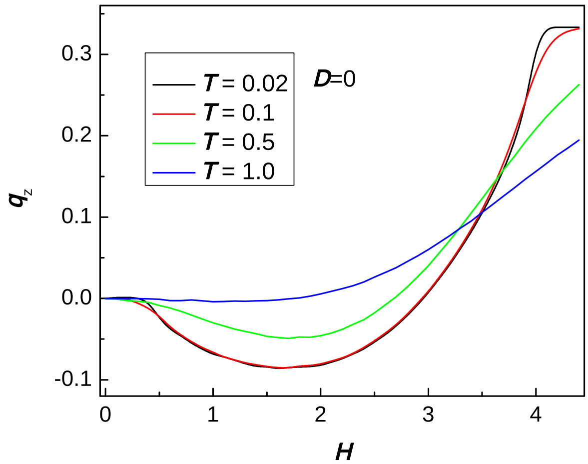

FIG. 10. The magnetic field behavior of the expectation value of the Stevens operator per site q_z at $D = 0$ for the pure Heisenberg case ($J' = 0$) of the spin-1 chain for several values of the temperature T.

phases is proportional to T^2 and inversely proportional to the Fermi velocity of the (gapless) elementary excitation. We emphasize (see Figs. 8–11) that the nonzero expectation value of the Stevens operator (the spin nematic ordering) for $D = 0$, caused by the external magnetic field, survives at nonzero temperatures for all values of the biquadratic exchange coupling.

In phases with gapped excitations (e.g., the spin-polarized phases, the large-D phases, and the Haldane phases), correlation functions decay exponentially as $\exp(-r\Delta_p/v)$, where Δ_p is the gap value and v is the velocity of the excitations related to the correlation function. In the framework of the conformal field theory it is possible to calculate the asymptotic behavior of correlation functions of one-dimensional quantum models in phases with gapless excitations [47]. Those correlation functions decay as $r^{-\eta_p}$, where the exponents η_p for integrable models can be calculated from the finite-size corrections [47]. For the considered model, two correlation

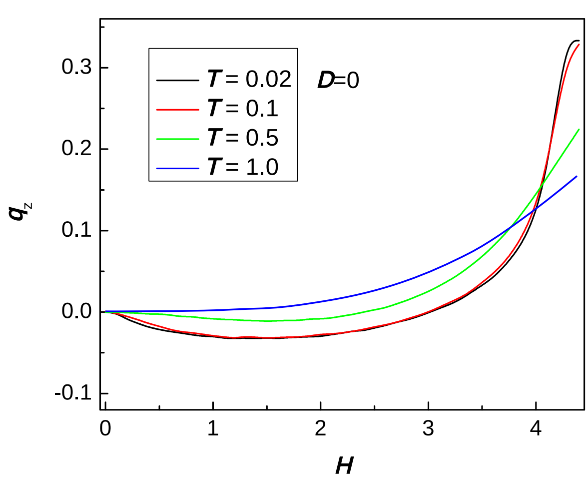

FIG. 11. The magnetic field behavior of the expectation value of the Stevens operator per site q_z at $D = 0$ for the case with negative biquadratic exchange $J' = -J/2$ of the spin-1 chain for several values of the temperature T.

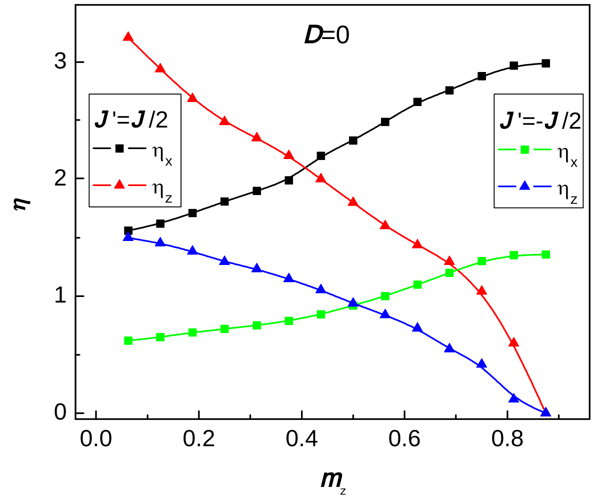

FIG. 12. The ground-state behavior of the exponents of the correlation functions of phases with gapless excitations as a function of the magnetic moment per site m_z for $D = 0$ and $J' = -J/2, J/2$: results of the exact diagonalization of 16 spins.

functions are important, namely,

$$\langle S_n^z S_{n+r}^z \rangle \propto r^{-\eta_z},$$
$$\langle (S_n^+)^2 (S_{n+r}^-)^2 \rangle \propto r^{-\eta_x}, \tag{10}$$

where $S_n^{\pm} = S_n^x \pm iS_n^y$, and $(S_n^+)^2(S_{n+r}^-)^2$ is obviously related to the correlation function of the Stevens operators $(O_2^0)_n(O_2^0)_{n+r}$. For nonintegrable models it is possible to calculate the related exponents using the exact diagonalization of finite chains [48].

Figure 12 manifests the behavior of related exponents $\eta_{z,x}$ as a function of the magnetic moment per site m_z (related to the applied magnetic field H). Exact results for the integrable cases $J = J'$ and $J = -J'$ qualitatively agree with the behavior presented in Fig. 12.

We see that for large m_z the dipole spin-spin correlations (with η_z) decay with distance more slowly than the quadrupole ones, while for small m_z the situation is the opposite.

V. INTERACTION WITH THE ELASTIC SUBSYSTEM

Now we are in a position to calculate how the spin nematic ordering can appear in spin-1 chain materials. It is known that the single-ion magnetic anisotropy is caused by two factors. First, the crystalline electric field of nonmagnetic ions (ligands) surrounding the magnetic ion affects the orbital moment of the latter. Then the spin-orbit interaction taken in the lowest approximation yields the single-ion magnetic anisotropy [28].

Consider the situation in which the field D is caused by the related strain u of ligands of the elastic subsystem of the spin chain crystal, $D = au$, where a is the spin-elastic coupling parameter. The strain reduces the symmetry of the crystal surrounding the spin-1 magnetic ions, e.g., from cubic symmetry to tetragonal symmetry. Such a strain enlarges the energy of the system as $Cu^2/2$, where C is the related elastic modulus [49]. (Here, we consider the elastic subsystem classically and in the ground state, because the characteristic elastic energy, the Debye temperature, is much stronger than

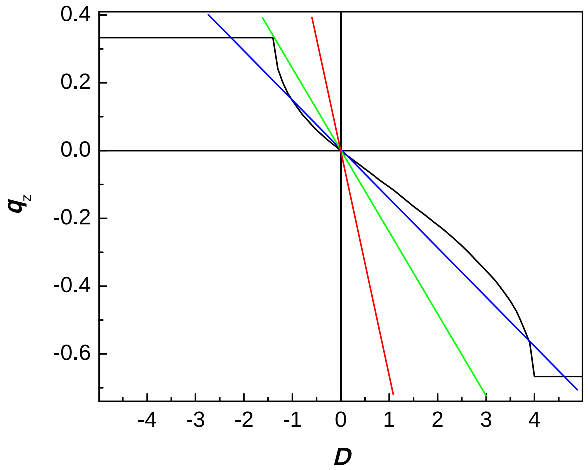

FIG. 13. The derivatives of the spin and the elastic contributions to the ground-state energy of the coupled spin-elastic subsystems for the SU(3) symmetric case at $H = 0$ as a function of D.

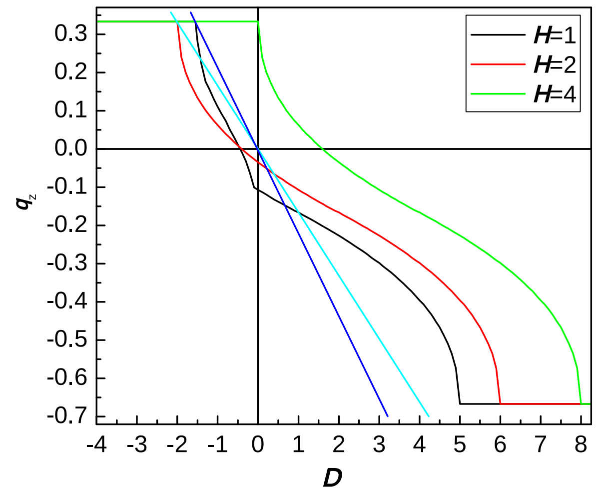

FIG. 14. The derivatives of the spin and the elastic contributions to the ground-state energy of the coupled spin-elastic subsystems for the SU(3) symmetric case for a nonzero value of the external magnetic field as a function of D.

the characteristic exchange coupling in spin chain materials.) Then the total Hamiltonian can be written as $\mathcal{H} + Cu^2/2$, in which $D = au$. For some values of the parameter D the energy of the spin subsystem becomes smaller than that at $D = 0$. Hence the nonzero strain produces the energy loss of the elastic subsystem and, at the same time, the energy gain in the spin subsystem of the crystal. The situation is similar to the Jahn-Teller effect (however, for the spin subsystem): The strain of the elastic subsystem, by reducing the symmetry, lifts the degeneracy of the spin subsystem, because in the absence of D the direction of the spin nematic order parameter is arbitrary. Taking into account that $q_z = N^{-1}\partial E/\partial D$, we plot in Fig. 13 the value of q_z, calculated using the exact Bethe ansatz solution, as a function of D at $H = 0$ together with the lines $-(C/a^2)D$ (the derivative of the elastic contribution to the energy with respect to D) for the SU(3) symmetric case.

We see that depending on the parameter $\alpha = C/a^2$, several situations can be realized. For small values of the coupling a or large values of the elastic modulus C the curve $q_z(D)$ crosses the lines $-\alpha D$ only at $D = 0$ (red line). In that case the system is in a situation in which the single-ion spin anisotropy cannot be realized. On the other hand, starting from some critical value of $\alpha_1 = 0.2357$ (notice that D is measured in units of J) the magnetic anisotropy appears: There is an intersection of the curve $q_z(D)$ with the line $-\alpha D$ (green line) at negative values of D.

Then we see that several intersections can exist for $\alpha < \alpha_1$ (blue line), which is typical for first-order phase transitions. It is clear that the magnetic anisotropy is related to the minimal contribution of the spin subsystem. For $\alpha \leqslant \alpha_2 = 0.156$ the intersections exist also for positive values of D.

Choosing the solution of the equation

$$q_z(D) = -\alpha D \tag{11}$$

(see Fig. 13) corresponding to the energy minimum, we find that for intermediate coupling the easy-axis magnetic anisotropy (with $D < 0$ and $q_z = 1/3$) is realized. For example, for $\alpha = \alpha_1$ there are two solutions: $D = -1$, corresponding to $q_z = 1/3$ with the energy $E/N \approx -1.886$ (in units of J), and $D = 0$, corresponding to $q_z = 0$ with the energy $E/N \approx -1.703$.

For smaller values of α, the easy-plane anisotropy appears (with $D > 0$ and $q_z = -2/3$). Actually, for $\alpha = \alpha_2$ there are three solutions: $D = -1$, corresponding to $q_z = 1/3$ with the energy $E/N \approx -2.219$; $D = 0$, corresponding to $q_z = 0$ with the energy $E/N \approx -1.703$; and $D = 4$, corresponding to $q_z = -2/3$ with the energy $E/N \approx -2.332$.

In Fig. 14 we show how the external magnetic field affects the spin nematic ordering caused by the interaction with the elastic subsystem in the ground state. Notice that the magnetic field itself can cause the spin nematic ordering without the coupling to the elastic subsystem; see above. The small magnetic field decreases the value of α_1; however, for $H > J$, it increases α_1. For $H \geqslant 4J$ the system is in the spin-polarized phase, in which $q_z = 1/3$.

A series of low-temperature dependencies $q_z(D)$, corresponding to different values of J', are presented in Fig. 15. These curves were obtained using the QMC method for systems with $N = 500$ spins, temperature $T = 0.05$, and $J' = 0, J/3, J/2, J$. As can be seen, the dependencies $q_z(D)$ for $J' \neq J$ are qualitatively similar to the case of $J' = J$, and hence the analysis of the solutions of Eq. (11) is similar to that considered above for the SU(3) symmetric case.

As can be seen from Fig. 16, at low temperatures the dependencies $q_z(D)$ are qualitatively similar to the case $T = 0$; thus solutions with nonzero q_z can exist, and we can use their analysis, analogous to the case of $T = 0$. On the other hand, with the increase in the temperature T the dependence $q_z(D)$ tends to a linear (paramagnetic) one. This means that for a fixed value of α there exists a critical temperature above which Eq. (11) has the only solution at $D = 0$.

It is important to point out that an effect similar to the effect of the strain of ligands can be realized for spin-1 bosons interacting with a Bose-Einstein condensate (BEC) [50]. Our theory can be applied to that situation too: In our notations, u plays the role of the respective component of the BEC, and

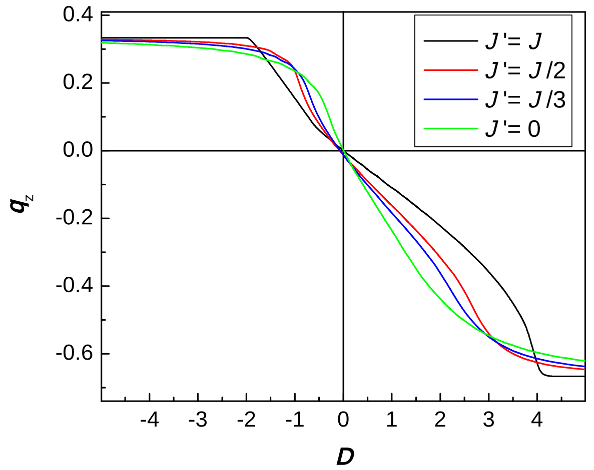

FIG. 15. The dependencies q_z on D, corresponding to different values of the parameter of the biquadratic exchange J', obtained using the QMC method for systems with $N = 500$ spins, temperature $T = 0.05$, and $J' = 0, J/3, J/2, J$.

as a result, the spin nematic ordering can take place. Such a situation can be realized in a system of spin-1 ultracold bosons situated in a one-dimensional optical lattice.

VI. HIGH-ENERGY PHYSICS APPLICATION

The exchange part of the SU(3) symmetric spin Hamiltonian can be written up to a constant as the permutation operator of the Gell-Mann matrices $\lambda_n^{a=1\cdots8}$ [$\mathrm{Tr}(\lambda^a\lambda^b) = 2\delta_{ab}$] [51], so that the SU(3) symmetric Hamiltonian can be written as

$$\mathcal{H} = \sum_n \left[J\frac{1}{2}\sum_{a=1}^{8} \lambda_n^a\lambda_{n+1}^a - H\lambda_n^2 + \frac{D}{\sqrt{3}}\lambda_n^8 + \frac{4J}{3}\right]. \qquad (12)$$

In fact, as in the spin-1 SU(3) symmetric chain, one can use any component of the SU(3) field (i.e., any $\sum_n \lambda_n^a$) in (12), which remains integrable; using the unitary transformation one can reduce the situation to (12). The components of the SU(3) fields (spin projections and Stevens operators) can be presented via Gell-Mann matrices. Namely, $\lambda^{7,5,2}$ are equal to S^x, $-S^y$, S^z operators, respectively, of the spin-1 projections; see, e.g., Ref. [50]. On the other hand, $\lambda^{1,4,6,3,8}$ are equal to the Stevens operators $-O_2^{-2}/2$, $-O_2^1/2$, $-O_2^{-1}/2$, $-O_2^2/2$, $\sqrt{3}O_2^0$, respectively [50]; sometimes other representations of the spin projection and quadrupole component operators are used. Notice that due to these relations, we see that $\lambda^{7,5,2}$ in the Hamiltonian (12) violate the time-reversal symmetry T, while $\lambda^{1,4,6,3,8}$ are related to the violation of the rotational symmetry O(3). In quantum chromodynamics (QCD), each Gell-Mann matrix is related to gluons [52], massless vector spin-1 gauge bosons with negative intrinsic parity, no electric charge, and no flavor, which participate in strong interactions, gluing quarks in hadrons. Matrices $\lambda^{1,2,4,5,6,7}$ describe color gluons, $g^1 = (r\bar{b} + b\bar{r})/\sqrt{2}$, $g^2 = -i(r\bar{b} - b\bar{r})/\sqrt{2}$, $g^4 = (r\bar{g} + g\bar{r})/\sqrt{2}$, $g^5 = -i(r\bar{g} - g\bar{r})/\sqrt{2}$, $g^6 = (b\bar{g} + g\bar{b})/\sqrt{2}$, $g^7 = -i(b\bar{g} - g\bar{b})/\sqrt{2}$. Here, r, g, b, $\bar{r}$, $\bar{g}$, $\bar{b}$ stand for red, green, and blue color and their anticolor counterparts. Matrices $\lambda^{3,8}$ are related to colorless gluons $g^3 = (r\bar{r} - b\bar{b})/\sqrt{2}$ and $g^8 = (r\bar{r} + b\bar{b} - 2g\bar{g})/\sqrt{6}$, which are antiparticles to themselves, i.e., they are true neutral particles. The singlet color state is forbidden. Gluons, which do not interact with quarks, are described by the SU(3) symmetric Yang-Mills theory [53]

$$\mathcal{L} = -\tfrac{1}{4}F_{\mu\nu}^a F^{a\mu\nu}, \qquad (13)$$

where the gauge invariant gluon field strength tensor is

$$F_{\mu\nu}^a = \partial_\mu \mathcal{A}_\nu^a - \partial_\nu \mathcal{A}_\mu^a + g f^{abc}\mathcal{A}_\mu^b\mathcal{A}_\nu^c, \qquad (14)$$

with $\mathcal{A}_\mu^a = A_\mu T^a$ (μ, ν are space-time variables, $a, b, c = 1, \dots, 8$) being the gluon fields related to the octet of generators of the SU(3) group $T^a = \lambda^a/2$, where $\mathrm{Tr}(T^aT^b) = (1/2)\delta_{a,b}$; g being the coupling strength constant (subject to the renormalization); and $f^{abc} = -(i/4)\mathrm{Tr}(\lambda^c[\lambda^a, \lambda^b])$ being the structure constants $[T^a, T^b] = if^{abc}T^c$. From this viewpoint the Hamiltonian (12) describes the one-dimensional quantum lattice toy model of interacting gluons. For that model we can use the results of previous sections with the obvious redefinitions $m_z \to N^{-1}\sum_n\langle\lambda_n^2\rangle$ and $q_z \to N^{-1}\sqrt{3}\sum_n\langle\lambda_n^8\rangle$, with H and D playing the role of the related components of (1 + 1)-dimensional Yang-Mills fields. Notice that from our results one can clearly see the difference in the behaviors of gluons, in particular, in different effects of the components of the Yang-Mills gluon fields on color gluons $g^{2,5,7}$, which components of the Yang-Mills field break the time-reversal T symmetry, and other color and colorless gluons, which components of the Yang-Mills field break the rotational O(3) symmetry, and in the different asymptotic behavior of correlation functions of such gluons. It is interesting that the external Yang-Mills field, which violates the time-reversal symmetry T, can cause the symmetry breaking for color and colorless gluons, which are not coupled to that field directly. The interaction of the spin subsystem with the elastic one for this high-energy model can be considered as the interaction of gluons with the Higgs-like field. Such a Higgs-like field plays the role of the strain of the elastic subsystem in the condensed matter model. The onset of the spin nematic ordering in the spin chain material is analogous to the

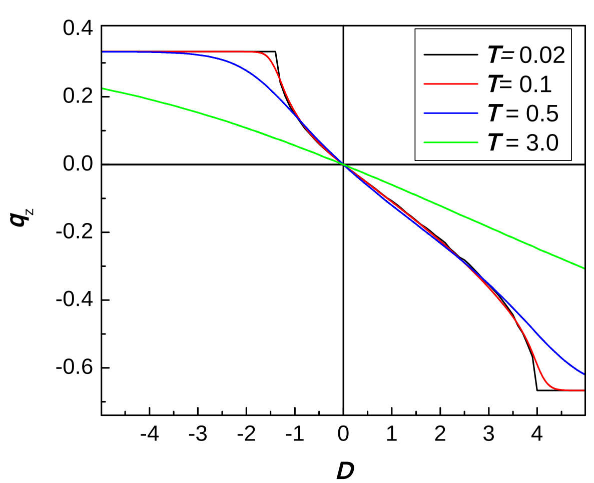

FIG. 16. The dependencies q_z on D, corresponding to different values of temperature T, obtained using the QMC method for systems with $N = 500$ spins and $J' = J$.

spontaneous symmetry breaking, e.g., for colorless interacting gluons in the toy model.

VII. SUMMARY

In summary, we have studied the onset of spin nematic ordering in the spin-1 chain material. The exact integrability for the SU(3) symmetric case and numerical simulations for various values of the biquadratic exchange interaction have permitted us to show that the external magnetic field can cause the spin nematic ordering in the ground state and at nonzero temperatures. On the other hand, we have studied the interaction of the spin subsystem with the elastic one. It is shown that such a coupling can cause the spin nematic ordering in the ground state and at low temperatures. The effect of the external magnetic field on that ordering has also been investigated. Our numerical results evidence that the spin nematic ordering in quasi-one-dimensional spin systems coupled with strains of the crystal lattice can take place for any value of the biquadratic exchange interaction. Our results can also be applied to the description of the onset of spin nematic ordering for systems of spin-1 ultracold bosons situated in one-dimensional optical traps, due to the coupling with a BEC. As a by-product, we discuss the obtained exact results in the framework of the SU(3) symmetric Yang-Mills-like toy theory of interacting gluons. We show that the Yang-Mills fields can cause symmetry breaking for gluons, which do not interact with those fields directly. Also, the interaction of gluons with the Higgs-like scalar field can cause spontaneous symmetry breaking in the gluon subsystem.

ACKNOWLEDGMENTS

A.A.Z. thanks N. Konik for helpful discussions. A.A.Z. acknowledges the support from SFB1143. V.V.S. acknowledges the support from the Pauli Ukraine Project, funded within the Wolfgang Pauli Institut Thematic Program "Mathematics-Magnetism-Materials (2021/2022)."

[1] P. G. de Gennes, *Liquid Crystals* (Clarendon, Oxford, 1974).
[2] L. D. Landau and E. M. Lifshitz, *Statistical Physics* (Elsevier, Amsterdam, 1980).
[3] R. Okazaki, T. Shibauchi, H. J. Shi, Y. Haga, T. D. Matsuda, E. Yamamoto, Y. Onuki, H. Ikeda, and Y. Matsuda, Science **331**, 439 (2011).
[4] M. P. Kolodyazhnaya, K. R. Zhekov, I. V. Bilych, G. A. Zvyagina, and A. A. Zvyagin, Fiz. Nizk. Temp. **43**, 1600 (2017) [Low Temp. Phys. **43**, 1276 (2017)].
[5] S. Kasahara, T. Shibauchi, K. Hashimoto, K. Ikada, S. Tonegawa, R. Okazaki, H. Shishido, H. Ikeda, H. Takeya, K. Hirata, T. Terashima, and Y. Matsuda, Phys. Rev. B **81**, 184519 (2010).
[6] R. Fernandes, A. Chubukov, and J. Schmalian, Nat. Phys. **10**, 97 (2014).
[7] S. Kasahara, H. J. Shi, K. Hashimoto, S. Tonegawa, Y. Mizukami, T. Shibauchi, K. Sugimoto, T. Fukuda, T. Terashima, A. H. Nevidomskyy, and Y. Matsuda, Nature (London) **486**, 382 (2012).
[8] X. Lu, J. Park, R. Zhang, H. Luo, A. H. Nevidomskyy, Q. Si, and P. Dai, Science **345**, 657 (2014).
[9] A. E. Böhmer and A. Kreisel, J. Phys.: Condens. Matter **30**, 023001 (2018).
[10] A. F. Andreev and I. A. Grishchuk, Sov. Phys. JETP **60**, 267 (1984).
[11] P. Chandra and P. Coleman, Phys. Rev. Lett. **66**, 100 (1991).
[12] A. V. Chubukov, Phys. Rev. B **44**, 4693(R) (1991).
[13] *Frustrated Spin Systems*, edited by H. T. Diep (World Scientific, Singapore, 2004).
[14] *Highly Frustrated Magnetism*, edited by C. Lacroix, P. Mendels, and F. Mila (Springer, Berlin, 2010).
[15] A. A. Zvyagin, Fiz. Nizk. Temp. **39**, 1159 (2013) [Low Temp. Phys. **39**, 901 (2013)].
[16] M. E. Zhitomirsky and H. Tsunetsugu, Europhys. Lett. **92**, 37001 (2010).
[17] N. Shannon, T. Momoi, and P. Sindzingre, Phys. Rev. Lett. **96**, 027213 (2006).
[18] H. T. Ueda and T. Momoi, Phys. Rev. B **87**, 144417 (2013).
[19] N. Büttgen, K. Nawa, T. Fujita, M. Hagiwara, P. Kuhns, A. Prokofiev, A. P. Reyes, L. E. Svistov, K. Yoshimura, and M. Takigawa, Phys. Rev. B **90**, 134401 (2014).
[20] A. Orlova, E. L. Green, J. M. Law, D. I. Gorbunov, G. Chanda, S. Krämer, M. Horvatić, R. K. Kremer, J. Wosnitza, and G. L. J. A. Rikken, Phys. Rev. Lett. **118**, 247201 (2017).
[21] M. Gen, T. Nomura, D. I. Gorbunov, S. Yasin, P. T. Cong, C. Dong, Y. Kohama, E. L. Green, J. M. Law, M. S. Henriques, J. Wosnitza, A. A. Zvyagin, V. O. Cheranovskii, R. K. Kremer, and S. Zherlitsyn, Phys. Rev. Research **1**, 033065 (2019).
[22] M. Blume and Y. Y. Hsieh, J. Appl. Phys. **40**, 1249 (1969).
[23] J. Stenger, S. Inouye, D. M. Stamper-Kurn, H.-J. Miesner, A. P. Chikkatur, and W. Ketterle, Nature (London) **396**, 345 (1998).
[24] E. Demler and F. Zhou, Phys. Rev. Lett. **88**, 163001 (2002).
[25] S. Nakatsuji, Y. Nambu, H. Tonomura, O. Sakai, S. Jonas, C. Broholm, H. Tsunetsugu, Y. Qui, and Y. Maeno, Science **309**, 1697 (2005).
[26] H. Tsunetsugu and M. Arikawa, J. Phys. Soc. Jpn. **75**, 083701 (2006).
[27] A. Läuchli, F. Mila, and K. Penc, Phys. Rev. Lett. **97**, 087205 (2006).
[28] See, e.g., A. A. Zvyagin, *Quantum Theory of One-Dimensional Spin Systems* (Cambridge Scientific, Cambridge, 2010).
[29] N. D. Mermin and H. Wagner, Phys. Rev. Lett. **17**, 1133 (1966).
[30] P. C. Hohenberg, Phys. Rev. **158**, 383 (1967).
[31] E. Barouch and B. M. McCoy, Phys. Rev. A **3**, 786 (1971).
[32] P. Pfeuty, Ann. Phys. (Amsterdam) **57**, 79 (1970).
[33] S. Sachdev, *Quantum Phase Transitions* (Cambridge University Press, Cambridge, 1999).
[34] G. V. Uimin, Pis'ma Zh. Eksp. Teor. Fiz. **12**, 332 (1970) [JETP Lett. **12**, 225 (1970)].
[35] C. K. Lai, J. Math. Phys. **15**, 1675 (1974).

[36] B. Sutherland, Phys. Rev. B **12**, 3795 (1975).
[37] J. B. Parkinson, J. Phys.: Condens. Matter **1**, 6709 (1989).
[38] H. Kiwata, J. Phys.: Condens. Matter **7**, 7991 (1995).
[39] A. Schmitt, K.-H. Mütter, and M. Karbach, J. Phys. A: Math. Gen. **29**, 3951 (1996).
[40] V. V. Slavin and A. A. Krivchikov, Low Temp. Phys. **40**, 985 (2014).
[41] A. W. Sandvik, Phys. Rev. B **59**, R14157(R) (1999).
[42] V. O. Cheranovskii, V. V. Slavin, E. V. Ezerskaya, A. L. Tchougréff, and R. Dronskowski, Crystals **9**, 251 (2019).
[43] V. O. Cheranovskii, V. V. Slavin, and D. J. Klein, Int. J. Quantum Chem. **121**, e26498 (2021).
[44] F. D. M. Haldane, Phys. Rev. Lett. **50**, 1153 (1983).
[45] H. Johannesson, Phys. Lett. A **116**, 133 (1986).
[46] L. Mezincescu, R. I. Nepomechie, P. K. Townsend, and A. M. Tsvelik, Nucl. Phys. B **406**, 681 (1993).
[47] See, e.g., A. A. Zvyagin, *Finite Size Effects in Correlated Electron Models: Exact Results* (Imperial College Press, London, 2005).
[48] T. Sakai, H. Nakano, R. Furuchi, and K. Okamoto, J. Phys.: Conf. Ser. **2164**, 012030 (2022).
[49] L. D. Landau and E. M. Lifshitz, *Elasticity Theory* (Pergamon, Oxford, 1984).
[50] M. S. Bulakhov, A. S. Peletminskii, S. V. Peletminskii, and Yu. V. Slyusarenko, J. Phys. A: Math. Theor. **54**, 165001 (2021).
[51] M. Gell-Mann, The eightfold way: A theory of strong interaction symmetry, Technical Report No. CTSL-20 TID-12608 (California Institute of Technology, Pasadena, 1961), doi: 10.2172/4008239.
[52] M. Creutz, *Quarks, Gluons, and Lattices* (Cambridge University Press, Cambridge, 1983).
[53] C.-N. Yang and R. L. Mills, Phys. Rev. **96**, 191 (1954).